Improvement of FEM's dynamic property*

Zeng-rong JIANG (江增荣)[1], Peng-fei DUAN (段鹏飞)[2],

Xing-lin GUO (郭杏林)[3], Hua DING (丁 桦)[2]

(1. The Second Research Department, Equipment Research Institute of PLA's

Second Artillery, Beijing 100085, P. R. China;

2. Institute of Mechanics, Chinese Academy of Sciences, Beijing 100190, P. R. China;

3. Department of Engineering Mechanics, Dalian University of Technology,

Dalian 116024, Liaoning Province, P. R. China)

(Communicated by Ya-pu ZHAO)

Abstract   The discretization size is limited by the sampling theorem, and the limit is one half of the wavelength of the highest frequency of the problem. However, one half of the wavelength is an ideal value. In general, the discretization size that can ensure the accuracy of the simulation is much smaller than this value in the traditional finite element method. The possible reason of this phenomenon is analyzed in this paper, and an efficient method is given to improve the simulation accuracy.

Key words   sampling theorem, efficiency, finite element discretization, macro element, condensation method, deformation modification, dispersion relationship

Chinese Library Classification   O242.21, O343, O241.81
2000 Mathematics Subject Classification   74S05, 74H15, 65N99

1   Introduction

The simulations of elasto-dynamics problems have various applications in engineering, and most of them need high efficiency in the calculation. For example, in the long-time simulation of the vibration problem of a large complex system, in the real-time simulation of a control system, etc., the efficiency of the calculation is always the key problem, especially the efficiency of every conventional time step. Therefore, the efforts of improving the calculation efficiency for the finite element method (FEM) have never been stopped, such as high-order elements[1], high precision time integration methods[2–4], mode superposition methods[5–6], dynamic substructure methods[6–8], and model reduction methods based on deformation modification[9–11]. All of them possess their own advantages and limitations. However, until now, few papers discuss why the size of the spatial discretization in the FEM is usually much smaller than the size needed by the sampling theorem (i.e., one half of the smallest wavelength), and whether there exists a better situation.

In this paper, this problem is discussed through the inertia moment analysis of a plan stress problem with a finite size domain, and a new marco element algorithm based on the FEM

is introduced as a way to approach the need of the sampling theorem by the analysis of the frequency dispersion properties of the algorithm.

2   Brief introduction of sampling theorem

As one of the most important rules on data discretization, the sampling theorem shows the conditions in which a continuous function can be accurately reconstructed by its discrete data. The specific description is given as follows.

For any continuous function $f(t)$, if its spectrum $F(\mathrm{i}\omega)$ has a finite bandwidth, i.e., there exists an upper limit $\omega_{\max}$ for the frequency such that $F(\mathrm{i}\omega) = 0$ for all $|\omega| \geqslant \omega_{\max}$, then $f(t)$ can be uniquely and completely reconstructed by its sampling values $f(nT)$ $(n = 0, \pm 1, \pm 2, \cdots)$ with the sampling frequency $\omega_{\mathrm{s}} \geqslant 2\omega_{\max}$ or the sampling length (often referred to as the sampling period in the time domain) $T \leqslant \pi/\omega_{\max}$

$$f(t) = \sum_{-\infty}^{+\infty} f(nT) \frac{[\sin \omega_{\mathrm{N}}(t - nT)]}{\omega_{\mathrm{N}}(t - nT)}, \tag{1}$$

where T is the sampling length, $\omega_{\mathrm{N}} = \omega_{\mathrm{s}}/2 = \pi/T$ is named as the Nyquist frequency, and the above reconstruction formula is called the Shannon formula.

The wavelength corresponding to the upper frequency limit $\omega_{\max}$ of $F(\mathrm{i}\omega)$ is $T_{\max} = 2\pi/\omega_{\max}$. Thus, the condition for Eq. (1) becomes $T \leqslant T_{\max}/2$, i.e., the sampling length should be less than or equal to one half of the wavelength.

Although the upper limit of the sampling length for completely reconstructing a continuous function $f(t)$ is $T_{\max}/2$ according to the sampling theorem, the sampling length that we usually use in practice is often much smaller than such an ideal value. This effect can be due to various reasons, such as the uncertainty of the highest frequency and the finite numbers of the sampling series.

In the traditional FEM for elasto-dynamics, the size of the spatial discretization is often from $1/10$ to $1/5$ of the smallest wavelength for implicit time integration, and from $1/10$ to $1/20$ for explicit time integration[12]. They are far away from the idea value $1/2$ given by the sampling theorem. The possible reason is discussed in this paper, and the highlight for improving the results is pointed out.

3   Discrete efficiency of FEM in elasto-dynamics

The calculation efficiency of the FEM depends on the discretization of both space and time, and the former is the focus of this paper.

It is known that, on the traditional FEM, only the deformation in the polynomial form can be exactly simulated, and the deformation in other forms, such as in the form of a trigonometric function, can only be approached by refining the mesh grids.

The wave propagation in an elastic body is the coupling phenomena of the elastic deformation effect and the inertial effect, and the extreme embodiment of this coupling effect is the propagation of harmonic waves. The efficiency of the discretization for the simulation of the elastic wave propagation can be described by the characteristic properties of the wave propagation of harmonic waves, which is just the extreme coupling relationship between the inertia and the deformation in a discrete model, namely, the relationship between the frequency and the wave number (for a given frequency, the wave number can be determined by the extreme coupling relationship). Eventually, the efficiency of discretization is depicted by the bias of the extreme coupling relationship between the discrete model and the continuous one. The bias is nothing but the frequency dispersion of the discrete model. Figure 1 shows the frequency dispersion for a four-node isoparametric element model[12–13]. Here, we express the relationship

with the function of the relative phase velocity and the relative discrete size for the convenience of discussion.

In Fig. 1, the relative errors of the elastic wave amplitude in the four-node isoparametric element model are about 20 corresponding to the Nyquist frequency $\omega_N = 0.5\,\omega_{max}$ ($dx/\lambda = 0.5$, where dx is the grid size, and λ is the wave length of the corresponding harmonic). One of the major causes of such errors should be that the shape functions of the finite element (FE) are generally piecewise polynomials with the compact support. However, the harmonics are the combination of the trigonometric functions with the infinite support, i.e., the support is the whole space. Inevitably, this disparity leads to the errors on the interpolation. Besides, the simulation of the inertia effect based on the shape function cannot ensure the effectiveness of the element angular momentum. At the same time, the element angular momentum has no constrains as the element translation momentums are constrained by the governing equations, and the error on the inertial moment is much larger than that on the inertial force (see Fig. 2). All of these lead to the final error.
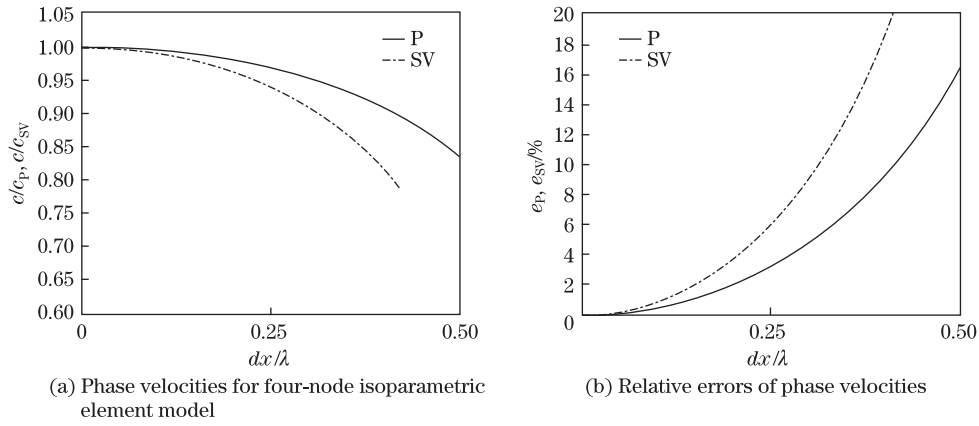

(a) Phase velocities for four-node isoparametric   (b) Relative errors of phase velocities
    element model

Fig. 1   Dispersion effect of four-node isoparametric element model
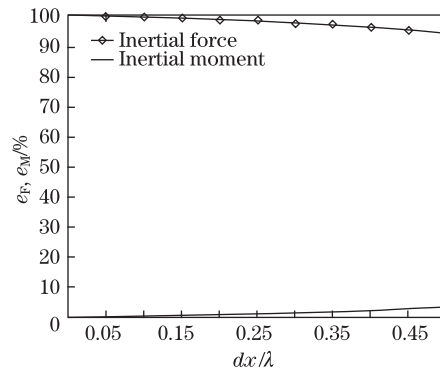

Fig. 2   Relative errors of inertial force and inertial moment for four-node isoparametric element

The simulation would get improvement in the condition of increasing the number of the element nodes (equivalent to the interpolation points). As an example, we consider a series of elements with a piecewise-polynomial shape function. The local internal moment is shown in Fig. 3. Here, the elements with the piecewise-polynomial shape function are equivalent to the composition of the isoparametric elements (see Fig. 4).

As shown in Fig. 3, for the fixed ratio of the size of the composite element and the harmonic wavelength, the approximation accuracy of the inertial moment increases with the number of the isoparametric elements within the composite elements. Simultaneously, the accuracy approaches the limit needed by the sampling theorem. In fact, for the construction of the composite element, increasing the number of the isoparametric elements is equivalent to refining the grid by the isoparametric elements. The discrete efficiency is not improved even though the approximation results are remarkably improved. In this case, the simulation accuracy of the deformation effect and the inertia effect is improved simultaneously. However, the cost is the increase of the system dimension. The introduction of the composite element brings us the following cognitions:

(i) In the simulation of the deformation caused by the harmonics, the efficiency of the polynomial based on the FE shape function is limited.

(ii) In the case of the composite element with refining the grids, the improvement on the approximations of the deformation and inertia effects is achieved at the same time, and consequently, it is not clear which one is more remarkable.
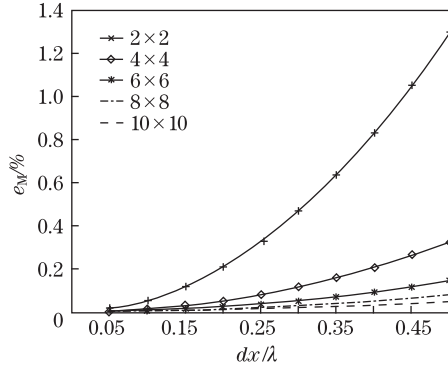

Fig. 3   Relative errors of inertial moment for composite element
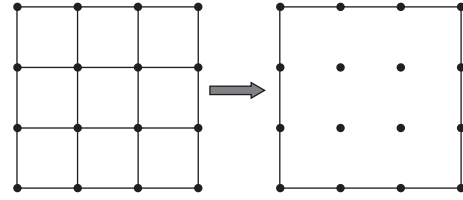

Fig. 4   Construction of composite element

Thus, the following questions are arised:

(i) Which kind of interpolation methods can be used to improve the approximation efficiency?

(ii) Is it possible to decouple the simulation of the two mechanical effects, deformation, and inertia to optimize the efficiency of the simulation by finding a good match for them?

In the following, the questions are discussed by taking advantage of the macro element algorithm based on the deformation modification[11].

4   Efficient dynamic analysis method based on FEM

To realize the decoupling of the two mechanical effects, under the condition of keeping the calculation in a certain scale (or the dimension of the system), we introduce the overall degrees of freedom (DOFs) of translation and rotation of the element mass points (DOFs of the centroid of the element, referred to as the centroid node) to describe the inertia effect of the whole element and simultaneously depict the element deformation effect with the cooperation of the centroid node and massless boundary nodes. In this way, a semi-decoupling of the two mechanical effects is realized so that we can improve the approximation of the deformation effect with increasing the number of the massless boundary nodes in the premise that the description of inertia effects remains unchanged, and the inertia effects are described by global momentum conservations. It should be pointed out that the DOFs of the boundary nodes can be reduced down before

solving the dynamic system. Therefore, in this point of view, the solution scale is just only related to the DOFs of the centroid nodes of the system.

4.1   Construction of macro element based on deformation modification

The condensation method based on the deformation modification is used to construct our macro element model. The outline of the method is as follows: Under the assumption of synchronizing movement, the full-size FE model of a structure is divided into several parts. The movement of each part is then approximated in a same pattern using a certain displacement model (such as the rigid movement model). By the minimization of the strain energy, an optimized displacement model can be established. Finally, the equations with the reduced total number of the DOFs are obtained[10–11].

For the macro element, one macro element can be regarded as a synchronistic part, and this sub-domain is demanded to keep all the boundary nodes of the original FE model. Hence, the displacement of the macro element is denoted with the cooperation of a pseudo rigid displacement model and the boundary displacement. Then, we obtain the optimized displacement distribution of the macro element through the deformation modification process and the displacement match of the boundary nodes. Furthermore, the inertia effects are concentrated on the DOFs of the centroid node. Figure 5 illustrates the construction of the macro element from its original FE model, in which the solid nodes represent the nodes with mass, whereas the boundary nodes of the element represent the massless nodes. Moreover, the shape of the element can be arbitrary in theory. The specific steps are as follows (also taking the plane stress problem as an example).
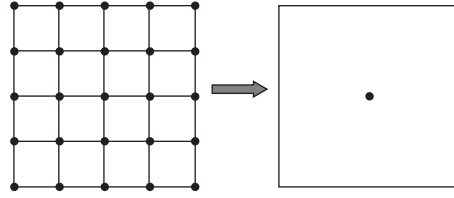

Fig. 5   Construction of macro elements

First, we introduce the rigid-body mode

$$\boldsymbol{u}_j = \begin{bmatrix} u_{jx} \\ u_{jy} \end{bmatrix} = \begin{bmatrix} 1 & 0 & -y_{cj} \\ 0 & 1 & x_{cj} \end{bmatrix} \begin{bmatrix} q_x \\ q_y \\ q_\phi \end{bmatrix} = \boldsymbol{R}_j \boldsymbol{q}_{\mathrm{m}} \tag{2}$$

for the entire macro element area under the assumption of synchronizing movement, where $\boldsymbol{u}_j$ represents the approximation of the displacement vector of node j, $\boldsymbol{q}_{\mathrm{m}}$ is the introduced rigid-body mode of the domain, $\boldsymbol{R}_j$ is the representation matrix of the three rigid body modes of node j (namely, the displacement approximation matrix), and x_{cj} and y_{cj} are the local coordinates of the node j related to the mass centre. We suppose that there are n nodes within the domain. The displacement vector of the domain, following the internal and external positions, can be defined as

$$\boldsymbol{u} = \begin{bmatrix} \boldsymbol{u}_{\mathrm{i\_1}} \\ \vdots \\ \boldsymbol{u}_{\mathrm{i\_}n} \\ \boldsymbol{u}_{\mathrm{b}} \end{bmatrix} = \begin{bmatrix} \boldsymbol{R}_1 \\ \vdots \\ \boldsymbol{R}_n \\ & & I \end{bmatrix} \begin{bmatrix} \boldsymbol{q}_{\mathrm{m}} \\ \boldsymbol{u}_{\mathrm{b}} \end{bmatrix} = \boldsymbol{R}\boldsymbol{q}, \tag{3}$$

where subscripts i and b signify, respectively, the characters of the inner and boundary nodes, and $\boldsymbol{R}$ and $\boldsymbol{q}$ are, respectively, the overall displacement approximation matrix and the modal

displacement vector representing the global translation and rotation of the domain. Then, we seek out the optimum vector q that can minimize the strain energy of the displacement difference $\delta u = u - \bar{u}$ between the FEM model and the macro element model. This is the so-called deformation modification process, which leads to an optimized relationship between the displacement corresponding to the original FE grid and the displacement vector of the macro element

$$u = K^{-1}((R^{\mathrm{T}}R)^{-1}R^{\mathrm{T}})^{\mathrm{T}}R^{\mathrm{T}}KRq = Tq. \tag{4}$$

Here, K is the original FE stiffness matrix of the domain, and T represents the overall displacement approximation matrix after the deformation modification. Following the node location order, the transforming formula of the displacement can be represented as

$$u = \begin{bmatrix} u_{\mathrm{i}} \\ u_{\mathrm{b}} \end{bmatrix} = Tq = \begin{bmatrix} T_{\mathrm{ii}} & T_{\mathrm{ib}} \\ T_{\mathrm{bi}} & T_{\mathrm{bb}} \end{bmatrix} \begin{bmatrix} q_{\mathrm{i}} \\ q_{\mathrm{b}} \end{bmatrix}. \tag{5}$$

By solving the second equation of Eq. (5), the approximate transformation formula of the macro element displacement vector $\begin{bmatrix} q_{\mathrm{i}} \\ u_{\mathrm{b}} \end{bmatrix}$ and the original FE $\begin{bmatrix} u_{\mathrm{i}} \\ u_{\mathrm{b}} \end{bmatrix}$ can be obtained as

$$\begin{bmatrix} u_{\mathrm{i}} \\ u_{\mathrm{b}} \end{bmatrix} = T_n \begin{bmatrix} q_{\mathrm{i}} \\ u_{\mathrm{b}} \end{bmatrix}, \tag{6}$$

where $T_n = \begin{bmatrix} T_{\mathrm{ii}} - T_{\mathrm{ib}}T_{\mathrm{bb}}^{-1}T_{\mathrm{bi}} & T_{\mathrm{ib}}T_{\mathrm{bb}}^{-1} \\ 0 & I \end{bmatrix}$.

The stiffness matrix of the macro element $K_{\mathrm{s}}^{\mathrm{e}} = T_n^{\mathrm{T}}KT_n$ (here, T_n^{T} is the transpose matrix of T_n) can be represented as

$$K_{\mathrm{s}}^{\mathrm{e}} = \begin{bmatrix} K_{\mathrm{sii}}^{\mathrm{e}} & K_{\mathrm{sib}}^{\mathrm{e}} \\ K_{\mathrm{sbi}}^{\mathrm{e}} & K_{\mathrm{sbb}}^{\mathrm{e}} \end{bmatrix} \tag{7}$$

following the node location order.

Finally, by lumping the total mass of the domain to the centroid node, the lumped-mass matrix of the macro element model is

$$M_{\mathrm{s}}^{\mathrm{e}} = \begin{bmatrix} M_{\mathrm{sii}}^{\mathrm{e}} & 0 \\ 0 & 0 \end{bmatrix} \tag{8}$$

with

$$M_{\mathrm{sii}}^{\mathrm{e}} = \begin{bmatrix} m & 0 & 0 \\ 0 & m & 0 \\ 0 & 0 & J \end{bmatrix}, \tag{9}$$

where m is the total mass of the domain of the macro element, and J is the inertia moment relative to the centroid node of the domain.

For a complex structure, we can discrete the solution domain with the macro element model (see Fig. 6) and then assemble the matrices of the physical effects with the same way as in the FEM. During the course, for convenience, the DOFs of the centroid nodes are placed on the top of the total displacement vector, which makes

$$M_{\mathrm{s}}\ddot{q} + K_{\mathrm{s}}q = F_{\mathrm{s}}, \tag{10}$$

where $\boldsymbol{q} = \begin{bmatrix} \boldsymbol{q}_{\mathrm{I}} \\ \boldsymbol{q}_{\mathrm{B}} \end{bmatrix}$ is the global displacement vector, $\boldsymbol{F}_{\mathrm{s}}$ is the global external force vector, and the global stiffness matrix is

$$\boldsymbol{K}_{\mathrm{s}} = \begin{bmatrix} \boldsymbol{K}_{\mathrm{sII}} & \boldsymbol{K}_{\mathrm{sIB}} \\ \boldsymbol{K}_{\mathrm{sBI}} & \boldsymbol{K}_{\mathrm{sBB}} \end{bmatrix}. \tag{11}$$

The global mass matrix is

$$\boldsymbol{M}_{\mathrm{s}} = \begin{bmatrix} \boldsymbol{M}_{\mathrm{C}} & \boldsymbol{0} \\ \boldsymbol{0} & \boldsymbol{0} \end{bmatrix} \tag{12}$$

with

$$\boldsymbol{M}_{\mathrm{C}} = \begin{bmatrix} \boldsymbol{M}_{\mathrm{sii}}^{\mathrm{e}} & & \\ & \ddots & \\ & & \boldsymbol{M}_{\mathrm{sii}}^{\mathrm{e}} \end{bmatrix}. \tag{13}$$

Here, subscripts I and B represent, respectively, the characters of the inner and boundary nodes of the system.

By Guyan's reduction method, the DOFs of massless nodes can be reduced, and we obtain the centroid lumped-mass macro element model (see Fig. 7) as follows:

$$\boldsymbol{M}_{\mathrm{C}} \ddot{\boldsymbol{q}}_{\mathrm{I}} + \boldsymbol{K}_{\mathrm{C}} \boldsymbol{q}_{\mathrm{I}} = \boldsymbol{F}_{\mathrm{I}} \tag{14}$$

with

$$\boldsymbol{K}_{\mathrm{C}} = \boldsymbol{K}_{\mathrm{sII}} - \boldsymbol{K}_{\mathrm{sIB}} \boldsymbol{K}_{\mathrm{sBB}}^{-1} \boldsymbol{K}_{\mathrm{sBI}}.$$
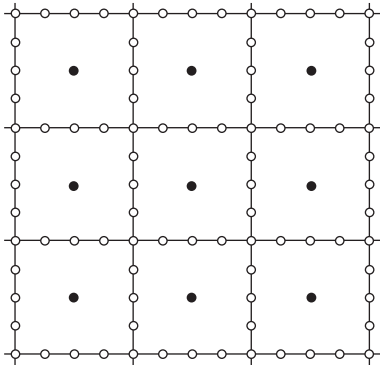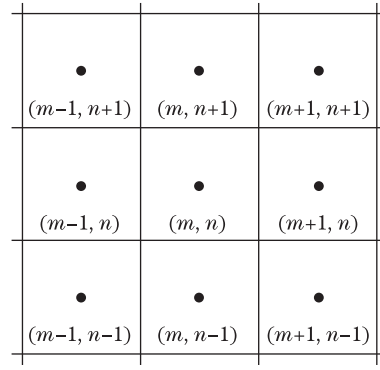

Fig. 6   Discretization by macro elements

Fig. 7   The lumped-mass model of macro element system

It should be noted that the information of the boundary condition has been included in $\boldsymbol{F}_{\mathrm{I}}$, and we will not discuss it since the following application does not involve it. Further study shows that the matrix $\boldsymbol{K}_{\mathrm{C}}$ is diagonally dominant. Thus, the movement of the centroid node (m, n) is almost only influenced by the nearest one. The actual calculations show that the movement of the centroid node (m, n) is almost not affected by the movement of the centroid nodes $(m + r, n + s)$ when $|r| > 2$ and $|s| > 2$, since the values of the related matrix elements have a difference of several orders in magnitude.

4.2   Influence of massless boundary nodes on frequency dispersion relationship

The macro elements of different numbers of boundary nodes can be obtained by discretizing the macro element domain with the consistent but different ways of the FE discretization. Figure 8 illustrates the three cases of the lumped-mass form of the macro element with different numbers of boundary nodes for a given domain, say, the macro element with 12, 16, and 20 boundary nodes. These different macro element models can be unified into the same form of the lumped-mass model.
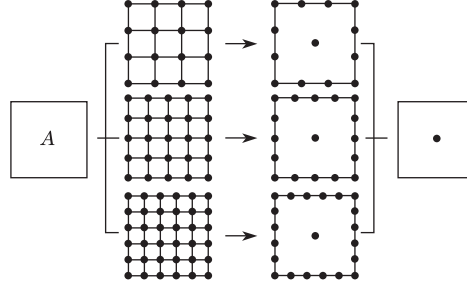

Fig. 8   Lumped-mass form of macro element with different numbers of boundary nodes

Different macro element models can be obtained with different ways of the FEM discretization. Then, the structure can be discretized with these macro element model which lead to different systems in the form of Eq. (10). However, by the condensation of reducing the DOFs of the massless boundary nodes, we can obtain the dynamic systems in the form of Eq. (14) with the same DOFs.

Following the traditional harmonic analysis, the plane harmonic solution to Eq. (14) can be assumed to take the form

$$\boldsymbol{q}(m, n) = \boldsymbol{q}_0 \exp[\mathrm{i}(\omega t - k_1 m dx - k_2 n dy)]. \tag{15}$$

Here, $\boldsymbol{q}_0$ is the amplitude vector of the centroid node $(0, 0)$, ω is the circular frequency, and $k_1 = k \cos \theta$ and $k_2 = k \sin \theta$ are still taken as the wave numbers, where k is the wave number, and θ is the wave propagation direction. Then, the amplitude of the other centroid nodes around (m, n) can be taken as

$$\boldsymbol{q}(m + r, n + s) = \boldsymbol{q}(m, n) \exp[\mathrm{i}(-k_1 r \Delta x - k_2 s \Delta y)]. \tag{16}$$

Further deduction leads to

$$\omega^2 \boldsymbol{M}^{\mathrm{e}}_{(m,n)} \boldsymbol{q}(m, n)$$
$$- \sum_{r=-\infty}^{+\infty} \sum_{s=-\infty}^{+\infty} \exp[\mathrm{i}(-k_1 r dx - k_2 s dy)][k_{\mathrm{e}}(m + r, n + s)] \boldsymbol{q}(m, n) = 0. \tag{17}$$

In short,

$$[\boldsymbol{W}_{(m,n)}]_{3 \times 3} \boldsymbol{q}(m, n)_{3 \times 1} = \boldsymbol{0}_{3 \times 1}.$$

Equation (17) is nothing but the equations of centroid motion of the element (m, n). The sufficient and necessary condition for the nonzero solution to Eq. (17) is that the determinant of its coefficient matrix equals zero, i.e.,

$$\det(\boldsymbol{W}_{(m,n)}) = 0. \tag{18}$$

Equation (18) is then the dispersion equation for the SV and P waves of the macro element discrete model.

Figure 9 shows the errors of the phase velocity of a plane harmonic propagation along the direction of $45°$ in the lumped-mass macro element models with different numbers of massless boundary nodes, where $dx/dy = 1$, and Poisson's ratio $\mu = 0.25$. It can be obviously observed that the increase of the number of the boundary nodes can remarkably improve the frequency dispersion behavior, and this improvement is very notable for the middle and high frequency phases.
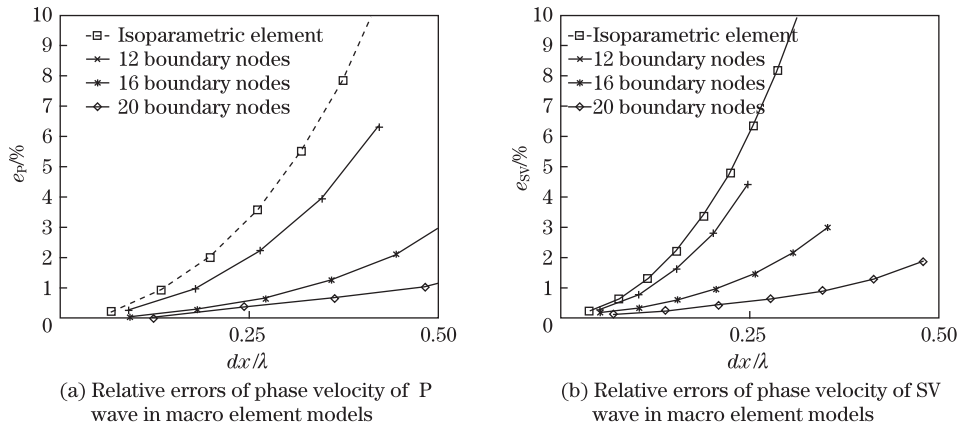

(a) Relative errors of phase velocity of P wave in macro element models

(b) Relative errors of phase velocity of SV wave in macro element models

Fig. 9   Effect of massless boundary nodes on dispersion relationships

Since the DOFs of the boundary nodes have been reduced down before the time integration, the final system scale is independent of the number of the boundary nodes. The above dispersion results indicate that, in the macro element method, the accuracy of the solution can be improved continuously in the condition of keeping the system DOF unchanged.

From Fig. 9(a), if we set the allowed accuracy as 1%, the ratio of the discrete size to the wavelength for the 20 boundary nodes model is nearly the idea value of the sampling theorem.

5   Conclusions and discussions

According to the above results, the following conclusions can be obtained:

(i) In the simulation of wave propagation by the traditional FEM, the performance of the rotational inertia effect simulation is very poor. This can be improved by refining mesh grids, but it sacrifices the sharp increase in the system scale, especially to the multi-dimensional problems.

(ii) The lumped-mass macro element introduces the translation and rotation DOFs of the centroid node, and it simulates efficiently the inertial effect of the whole element and, at the same time, realizes the semi-decoupling of the deformation and inertia effects of the element.

(iii) By this decoupling character, the macro element method realizes the non-synchronization in the improvement of the inertia and deformation effects. Thus, in the condition of keeping the system DOF unchanged, we can improve the accuracy of the wave simulation continuously in a certain condition (at least the restriction of the sampling theorem).

(iv) The construction of the macro element signifies its extensive applicability. As it is based on the FEM, it requires nothing special in the space dimension, shape, or even the selection of the synchronizing displacement mode.

The results of this paper show the potentiality of the introduced method. There is a lot of work to be done before its practical application. Meantime, further improvement of the method

is still needed. We hope that this paper will start a discussion.

References

[1] Zienkiewicz, O. C. and Taylor, R. L. *The Finite Element Method* (in Chinese), 5th Ed., Tsinghua University Press, Beijing (2008)

[2] Zhong, W. X. On precise time-integration method for structural dynamics (in Chinese). *Journal of Dalian University of Technology* **34**(2), 131–136 (1994)

[3] Zhong, W. X. Precise computation for transient analysis (in Chinese). *Computational Structural Mechanics and Applications* **12**(1), 1–6 (1995)

[4] Wang, M. F. and Au, F. T. K. Higher-order schemes for time integration dynamic structural analysis. *Journal of Sound and Vibration* **277**(3), 122–128 (2004)

[5] Zhao, Y. Q. and Liu, Z. S. Modal truncation and the response sensitivity to harmonic excitation (in Chinese). *Computational Structural Mechanics and Applications* **13**(3), 313–319 (1996)

[6] Xiang, S. H., Qiu, J. B., and Wang, D. J. The resent progresses on modal analysis and dynamic sub-structure methods (in Chinese). *Advances in Mechanics* **34**(3), 289–303 (2004)

[7] Wang, Y. Y. *Method of Dynamic Sub-structure: Theory and Application* (in Chinese), Science Press, Beijing (1999)

[8] Lou, M. L. *Sub-structure Method in Structural Dynamic Analysis* (in Chinese), Tongji University Press, Shanghai (1997)

[9] Liu, B., Ding, H., and Shi, Z. M. A model reduction method for dynamic analysis based on quasi-rigid-body mode and flexibility modification (in Chinese). *Engineering Mechanics* **24**(10), 25–29 (2007)

[10] Zheng, S. F. and Ding, H. A model reduction method for dynamic analysis based on deformation modification and local rigid body mode (in Chinese). *Mechanics in Engineering* **30**(6), 31–34 (2008)

[11] Zheng, S. F. *A Model Reduction Method and Its Application for Dynamic Analysis Based on Deformation Modification and Local Rigid Body Mode* (in Chinese), Ph. D. dissertation, Institute of Mechanics, Chinese Academy of Sciences (2009)

[12] Liu, J. B. *Wave Motion in the Finite Element Simulation and the Influence of Complex Field on the Earthquake Motion* (in Chinese), Ph. D. dissertation, Institute of Engineering Mechanics, China Earthquake Administration (1990)

[13] Liu, J. B. and Liao, Z. P. In-plane wave motion in finite element model. *Acta Mechanica Sinica* **8**(1), 80–87 (1992)

[14] Duan, P. F. *On Dispersive Properties of Macro-element Algorithm on Deformation Modification* (in Chinese), Ph. D. dissertation, Institute of Mechanics, Chinese Academy of Sciences (2010)